ADVANCED OPTICAL MATERIALS
www.advopticalmat.de

Disrupting J-Aggregation in Triazatruxene Dimers to Develop Responsive Luminescent Inks for Anti-Counterfeiting Applications

*Raúl Martín, Marcelo Echeverri, Francisco González, Alicia de Andrés, M. Carmen Ruiz Delgado, Alberto Concellón, José Luis Serrano, and Berta Gómez-Lor**

The fight against counterfeiting is a crucial concern for economies around the world, underscoring the urgent need for effective measures to ensure the legitimacy of products and documents. Luminescent security inks have emerged as effective tools in this battle. The third generation of these inks, incorporating stimuli-responsive organic materials, enables unique efficiency. In this work, the stimuli-responsive behavior of three trialkylated triazatruxene dimers (TRI1, TRI2, and TRI3), endowed with *N*-alkyl chains of different length is investigated. Among them, TRI3, with three flexible dodecyl chains, shows remarkable stimuli-responsive fluorescence that is attributed to thermally or shear-induced phase transitions between a tetragonal columnar phase and a discotic-nematic liquid crystal phase. Such transformation involves the breakdown of highly emissive J-aggregates with a strong influence on the resulting emissive color. Interestingly, these stimuli-triggered transformations are spontaneously reversed, which renders this compound very interesting in the search of third-generation security inks.

1. Introduction

Counterfeiting represents a serious threat to businesses, consumers, and global economies. In an age of increasingly sophisticated counterfeiters, the importance of security features to preserve the integrity of products and documents cannot be overemphasized. Strong anti-counterfeiting elements ensure that consumers receive authentic products while safeguarding brand reputation and public safety.

One of the most effective solutions in this battle is the use of luminescent security inks,[1,2] which are specially formulated with unique features that make them difficult to reproduce but easy to recognize. To date, a variety of luminescence security inks has been developed based on different materials, including rare-earth metal complexes,[3,4] perovskites,[5] quantum dots,[6] carbon dots,[7] metal-organic frameworks,[8] polymers,[9] metal nanoclusters,[10] or organic dyes.[11]

Since the emergence of the first generation (invisible single luminophores in daylight that show bright emission under UV irradiation)[12] and second generation (multiple or single luminophores with more than one emission)[13] of security inks, stimuli-responsive materials have opened up a third generation of smart security inks.[8,14–17] These materials display unique responses in photoluminescence under the influence of stimuli such as light, electricity, heat, pressure, pH, gas, or water exposure, etc.

In the search for stimuli-responsive light-emitting materials, organic materials have a privileged position. Their light emission properties are closely related to the presence of delocalized π-electrons along the backbone of the molecule, with a strong dependence on the degree of π-conjugation.[18] Consequently, conjugated molecules featuring readily accessible conformers are of particular interest in the search for stimuli-responsive fluorophores. Additionally, the light-emitting properties of π-conjugated molecular solids and films are also strongly dependent on the supramolecular arrangement of the constituting molecular units. This strong dependence of the final material properties on the organization of the molecular building blocks at the nanometer level, presents numerous opportunities to

R. Martín, M. Echeverri, A. de Andrés, B. Gómez-Lor
Instituto de Ciencia de Materiales de Madrid
CSIC C/ Sor Juana Inés de la Cruz, 3, Madrid 28049, Spain
E-mail: bgl@icmm.csic.es

R. Martín, F. González
Faculty of Chemical Science and Technology
Instituto Regional de Investigación Científica Aplicada (IRICA)
University of Castilla-La Mancha
Ciudad Real 13071, Spain

M. C. Ruiz Delgado
Department of Physical Chemistry, University of Málaga
Campus de Teatinos s/n
Málaga 29071, Spain

A. Concellón, J. L. Serrano
Departamento de Química Orgánica
Instituto de Nanociencia y Materiales de Aragón (INMA)
CSIC-Universidad de Zaragoza
Zaragoza 50009, Spain

The ORCID identification number(s) for the author(s) of this article can be found under https://doi.org/10.1002/adom.202400965

DOI: 10.1002/adom.202400965

synthesize fluorescent materials capable of responding to external stimuli by varying their supramolecular arrangement.[19]

When conjugated molecules organize in the solid state, they tend to form H-type or J-type aggregates, depending on the relative alignment of their transition dipole moments. This alignment has significant implications for the energies of excited states and the oscillator strengths of transitions from the ground state to these excited states.[20] While cofacial π-stacked structures (H-aggregates) led to decreased blue-shifted emission, a head-to-tail arrangement of the molecules gave rise to red-shifted emissions (J-aggregates) with interesting optical properties (narrow red-shifted absorption bands, superradiance) and with the ability to delocalize excitons along numerous molecular units. These properties have aroused interest in various fields such as imaging[21] energy harvesting and photovoltaics[22,23] or biomedical applications.[24] On the other hand, the high sensitivity of the optical properties of J-aggregates to external influences has been successfully used in the development of efficient sensing and anticounterfeiting molecular systems.[24,25]

While the synthesis of stimuli-responsive security inks has made significant progress, the understanding of its microscopic behavior is still a challenge. Smart crystalline materials,[26] are the materials of choice to understand the response mechanism and to establish structure-property relationships at a molecular level by single-crystal analysis. Unfortunately, color changes between single-crystalline polymorphs are rather exceptional, for involving a transformation of the supramolecular and/or intramolecular structure within the constrained environment of the crystal. In addition, with few exceptions, organic single crystals are brittle, resulting in inhomogeneous films and hindering their processability. The soft character of liquid crystals has emerged as an attractive design in the search for smart materials due to their responsive and adaptive attributes and their easy processability from solution or a melt while providing interesting information on supramolecular arrangement.[27]

We have long been involved in the development of semiconducting triindole-based discotic liquid crystals. Triazatruxene (also known in the literature as triindole) is a heptacyclic molecule that exhibits interesting linear[28] and non-linear[29,30] optical properties. Due to its strong emission and high sensitivity to its environment, this aromatic platform has found applications in areas ranging from OLEDs,[31,32] cell imaging[33] to fluorescent sensors.[34,35]

On the other hand, we have previously found that dimerizing fluorophores via diacetylene bridges is an attractive design strategy in the construction of stimuli-responsive light-emitting materials.[36] The low rotational barrier imposed by this linker allows for the easy modulation of the extension of the conjugation and electronic communication between the fluorophores. Additionally, its flexibility favors the easy modification of the local geometry of the molecules, potentially impacting how they interact with other molecules in the bulk. Both factors will have evident influences on their optical properties.

With these precedents in mind, this work investigates the stimuli-sensitive light-emitting properties of three trialkylated triazatruxene dimers labeled **TRI1**, **TRI2**, and **TRI3**. These dimers are constructed by connecting two triazatruxene units through a diacetylene bridge, and they differ in the length of the alkyl chains connected to the nitrogen functionalities (ethyl, hexyl, or dodecyl, respectively). The results indicate that the length of the alkyl chains significantly influences how these molecules assemble in the bulk, resulting in notable consequences for their responsiveness. In fact, only **TRI3**, endowed with three dodecyl flexible chains exhibits a stimuli-responsive fluorescence. This compound crystallizes forming brick-wall stacks as could be determined by single crystal analysis, with the molecules adopting a head-to-tail arrangement. The light emitting properties of **TRI3** significantly change under the influence of heat or pressure, which have been attributed to thermally or mechanically shearing-induced phase transitions between a tetragonal columnar and a discotic nematic liquid crystal phase. Such phase transformation involves the breakdown of highly emissive J-aggregates which is the origin of the drastic changes in the emitting color. These stimulus-triggered transformations are spontaneously reversible upon deposition on glass or paper, which is very interesting for their applications as third-generation security inks.

2. Results and Discussion

2.1. Synthesis and Photophysical Properties of TRI1-TRI3

The synthesis of **TRI1**-**TRI3** (**Figure 1**) involved the monobromination of the corresponding *N*-trialkyltriazatruxene, followed by Sonogashira coupling with TMS acetylene. Subsequent deprotection of the TMS group under basic conditions renders the corresponding monoethynyl derivative which was dimerized under Glaser homocoupling conditions (Scheme S1, Supporting Information). The synthesis and characterization of **TRI1** and **TRI2** can be found in the Supporting Information. **TRI3** has been previously reported by our group (Figure 1).[37]

The photophysical properties of these molecules were studied by UV–vis and fluorescence spectroscopy. The UV–Vis absorption spectrum of **TRI1**-**TRI3** at 1×10^{-5} M solution in $CHCl_3$ exhibits two predominant absorption bands localized at 320 and 398 nm. As previously described,[37] the lowest-energy electronic band corresponds to the HOMO-LUMO transition and it has a certain charge-transfer (CT) character from the peripheral electron-rich triazatruxene units to the central moderately electron-deficient diacetylene. The fluorescence spectra of the three compounds show a maximum emission wavelength of 458 nm (**Figure 2**b) and quantum yields of 0.55, 0.43, and 0.42 for **TRI1**, **TRI2**, and **TRI3**, respectively (Table S1, Supporting Information). In the solid state, the absorption spectra of **TR1** and **TR2** show a slight redshift, while **TR3** exhibits a narrow, intense new band at 450 nm. The emergence of narrow bands bathochromically shifted with respect to the isolated molecules is characteristic of J aggregation.[20,38]The fluorescence spectra of solid **TR1** and **TR2** experience red-shifts of ≈20 nm, whereas the emission maximum of **TR3** shifts to 500 nm.

The fluorescence of **TRI1**-**TRI3** was investigated in different solvents (see Figure S1 and Table S1, Supporting Information). All three compounds show a moderate solvent dependence with emission bands shifting bathochromically as the solvent polarity increased from hexane (≈430 nm) to dimethylformamide

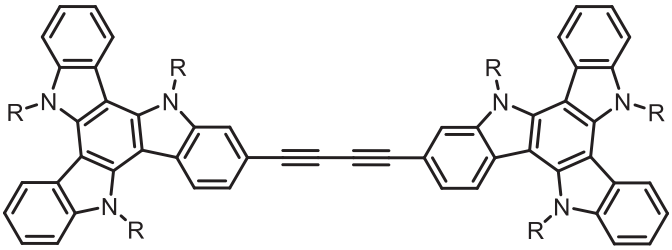

Figure 1. Chemical structure of **TRI1-TRI3**.

(≈470 nm). Two emission bands are found in no polar solvents (hexane and toluene) which comes with a loss of its fine vibronic structure as the solvent polarity increases. This is a typical signature of a fluorescence emission arising from a CT excited state.[39]

To shed light on the aggregation behavior of **TRI1-TRI3** of these compounds we recorded the fluorescence spectra in THF-water mixtures. The changes in water fraction versus fluorescence intensity were plotted in **Figure 3** and show that upon increasing the water fraction up to 50% for **TRI1**, 40% for **TRI2,** and 30% for **TRI3** respectively, the maximum emission intensity gradually increases. This observed effect of enhanced emission upon aggregation[40,41] could be explained on the basis of the restriction of intramolecular rotation as one of the most extended plausible mechanisms for aggregation-enhanced emissions.[42,43] Note that theoretical calculations predict a rather flat torsional potential for diacetylenic-bridged triindole dimers between the perpendicular conformation and the most stable trans-coplanar conformer (see Supporting Information).[37] The addition of water is expected to block the rotational motion of the molecule and thus reduce the non-radiative deexcitation pathways leading to enhanced emissions.

In all three cases after surpassing the above amounts of water the fluorescence is quenched. However, in compound **TRI3** after the initial PL decrease after adding 30% of water, a further increase in the water percentage, led to the emergence of a new red-shifted emission band again suggesting the formation of J-aggregates. In fact, the absorption spectra of **TRI3** confirm the emergence of the intense and sharp red-shifted absorption band characteristic of J-aggregates as the amount of water is increased (Figure S2, Supporting Information).

2.2. Crystal Growth and Structure Determination of TRI3

Compound **TRI1-TRI3** are obtained as yellow solids. Powder X-ray diffraction shows that, while **TRI1** and **TRI2** are amorphous

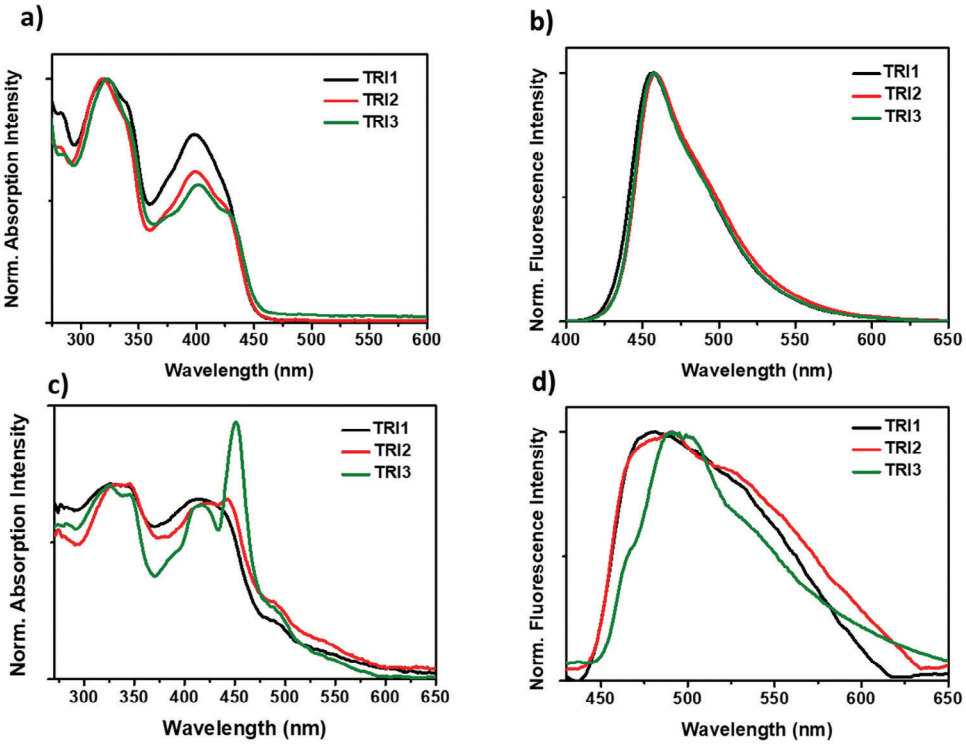

Figure 2. a) Normalized absorption and b) emission spectra of **TRI1-TRI3** in solution ($CHCl_3$, 1×10^{-5} M) and c) normalized absorption and d) normalized emission spectra in films upon excitation at 330 nm. Absorption has been normalized to the 330 nm band.

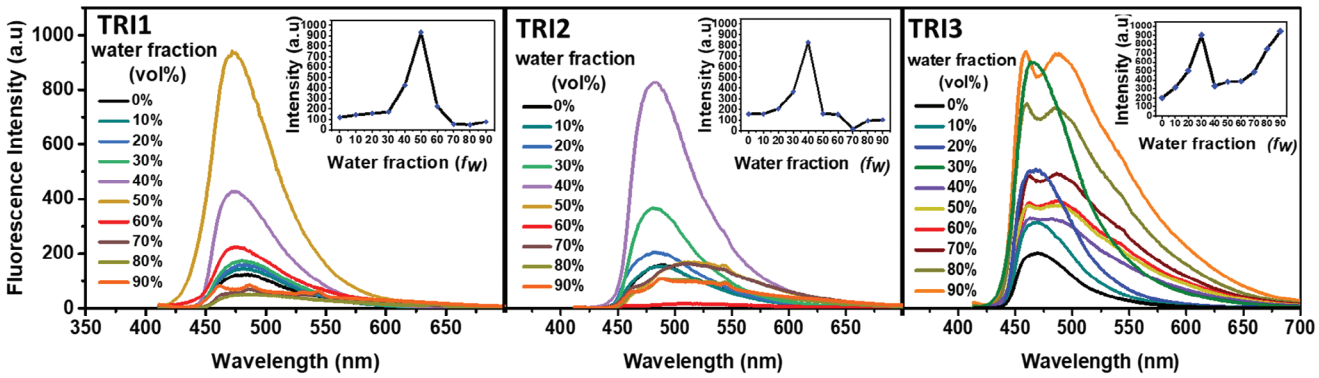

Figure 3. PL spectra of **TRI1-TRI3** in water/THF mixtures with different water fractions (f_w = 0–90%) (λ_{exc} = 330 nm). Inset, variation of the intensity of the maximum emission peak with the different water fractions.

materials, **TRI3** exhibits intense peaks indicative of a crystalline solid (Figure S5, Supporting Information). Soft yellow single crystals of **TRI3** were obtained by slow diffusion of a poor solvent (acetone) into a $CHCl_3$ solution which was suitable for X-ray crystal structure determination. This compound crystallizes in the triclinic space group P-1, with only half an independent molecule per unit cell. The alkyl chains experience disorder but could be successfully modeled with geometric constraints on two alternative sets of positions, particularly at the most disordered atoms. The triazatruxene units within the molecule display slight distortions, with the outer rings exhibiting torsion angles ranging from 2° to 9° with respect to the central ring. However, the two rings connected by the diethynyl bridge lie in the same plane (**Figure 4a**).

The molecules organize into columns, adopting a bricklayer stacking mode (Figure 4b), where each triazatruxene unit in the dimer forms part of a different column organizing in a head-to-tail manner. Considering that the molecular transition dipole moment accommodates along the long axis of the molecules, this arrangement explains the formation of J-aggregates.[44] The crystallographic packing is stabilized by CH-π interactions involving the central ring and the polarized CH_2 group attached to the nitrogen. We have previously found that CH-π interactions play a significant role, in the supramolecular arrangement of triazatruxenes both in solution[45] and in bulk.[46–48]Along the *c*-axis these stacks organize forming layers, separated by the alkyl chains that are strongly interdigitated (Figure 4c).

2.3. Study of the Stimuli-Responsive Emission Behavior

Considering the low rotational barrier imposed by the diethyl linker, which may influence not only the extent of molecule

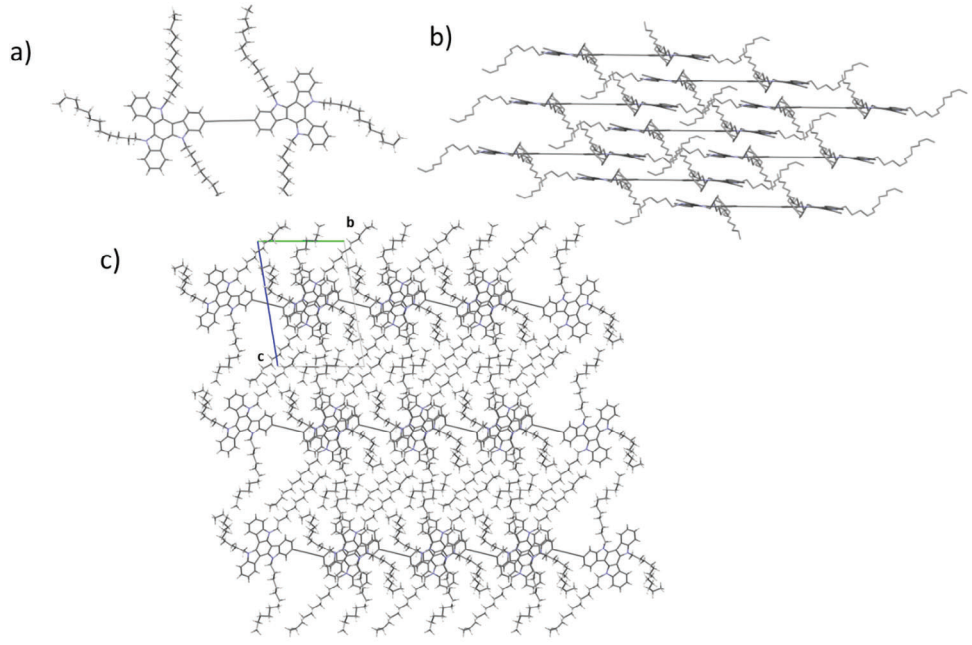

Figure 4. a) View of the molecule, showing only the highest occupancy atoms of the disordered alkyl chains. b) Lateral view of the bricklayer stacking arrangement. c) View of the crystal packing along *a* showing the layered arrangement of the stacks.

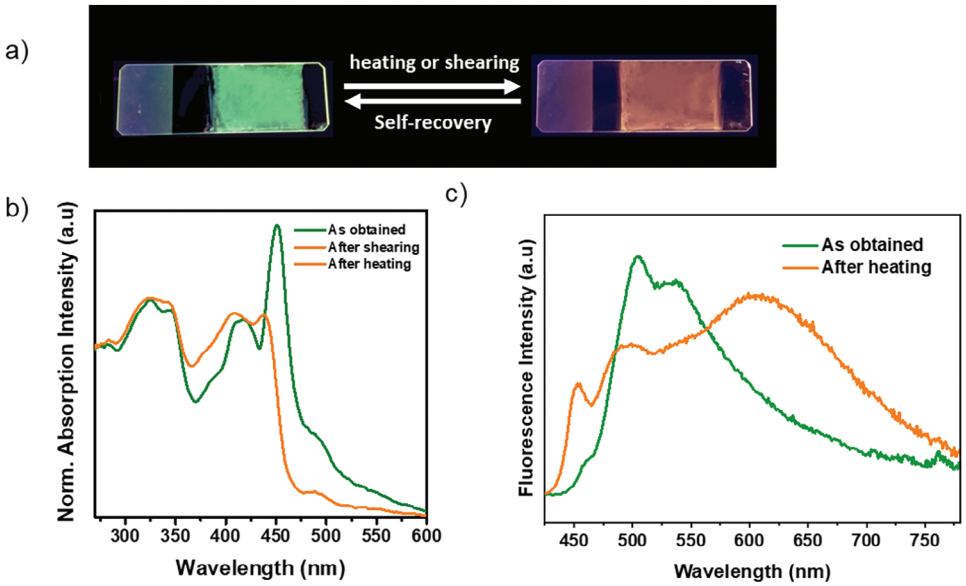

Figure 5. a) View of **TRI3** thin film under 365 nm light before and after thermal transformation. b) Absorption and c) fluorescence spectra ($\lambda_{exc} = 410$ nm) of thin film of **TRI3** as obtained and after the different external stimuli. Absorption spectra have been normalized to the 330 band.

conjugation but also the molecular geometry and subsequently how molecules interact with each other, we have investigated the responsive behavior of **TRI1**-**TRI3** thin films prepared by blade coating over glass slides.

Interestingly while compounds **TRI1** and **TRI2** do not show significant changes when heated or sheared, **TRI3** films experiment with a vivid color change from initial green to brownish when visualized under a UV lamp (**Figure** 5a). The changes in the optical properties were studied by UV absorption and fluorescence spectroscopy (Figure 5b,c). The UV spectra of the transformed films (Figure 5b) show a clear decrease in the intense narrow peak attributed to the J-aggregation, suggesting the breakage of this arrangement after the external perturbation.

The different spectra have been deconvoluted to shed light on the different light-emitting species in the pristine and the transformed films, which show the contribution of four species centered at 460, 500, and 600 nm and attributed to the free exciton, the J-aggregate and two tentatively assigned exciton-trapping excimer-like species. Details of the different coexisting bands are given in the Supporting Information. Comparison of the fluorescence spectra before and after shearing/ heating, show a significant decrease of the main band at 500 nm, an increase of the blue-shifted peak ≈460 nm, and a broad red-shifted band ≈600 nm. Thus, the apparent color change upon thermal or shear stimulation is in fact, the result of a change of the relative weight of the different components in the emission spectra, due to J- aggregation disruption and an increase in the population of the monomeric and cofacial aggregates.

Interestingly the emission transformation is completely spontaneously recovered after ≈60 min (Figure S3, Supporting Information).

This behavior allowed us to draw different motifs on **TRI3** films by shearing with a spatula or approaching a heated steel stamp that spontaneously is erased after a period of time (**Figure** 6). The transformation at the micro-scale was studied by recording the micro-photoluminescence and micro-transmittance spectra of the written and non-written regions of the films using a laser line at 488 nm (see Figure S4, Supporting Information) and similar results were obtained within the 5 µm areas explored.

This stimuli-responsive behavior was studied more in-depth by employing a combination of powder X-ray diffraction (PXRD), polarizing optical microscopy (POM), and differential scanning calorimetry (DSC).

Observation of thin films of **TRI3** under a microscope equipped with crossed polarizers revealed a birefringent texture typical of columnar liquid crystals (**Figure** 7a), indicating the existence of a liquid crystal phase due to material's fluidity. Powder X-ray diffraction patterns of the films showed the

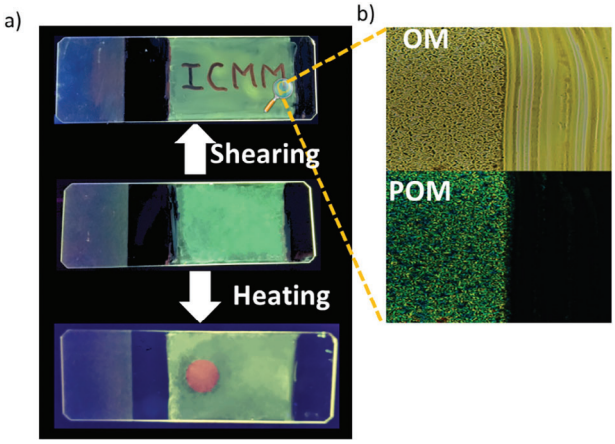

Figure 6. a) View of **TRI3** thin film over glass, showing different motifs by shearing or thermal treatment. Images visualized under 356 nm light. b) Optical microscopy photographs under visible and polarized light of the frontier of a non-written/written region of a thin film of **TRI3**.

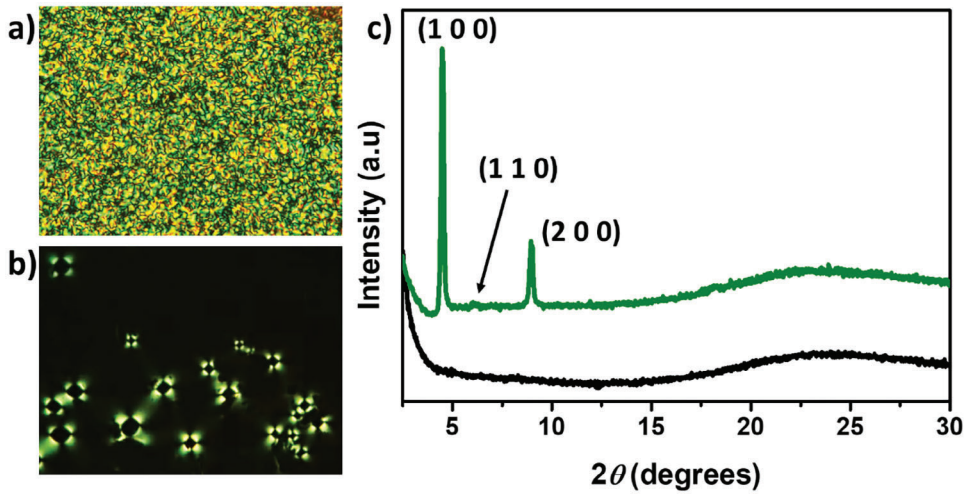

Figure 7. View of the POM textures of **TRI3** a) as obtained and b) after shearing. c) PXRD of the thin films of **TRI3** as obtained (green line) and after shearing (black line).

presence of three low-angle peaks with *d*-spacings in the ratio of $1:1/\sqrt{2}:1/\sqrt{4}$ arising from the (100), (110), and (200) reflections of a tetragonal columnar phase (Figure 7c). We note that the (110) reflection has a considerably lower intensity in comparison to the (100) and (200) ones, and indeed (110) is observed as a shoulder. This low intensity in the (110) reflection has also been observed in several tetragonal columnar phases.[49,50] The good match of the peaks at low angles with those of the powder X-ray diffractogram simulated from the single crystal data suggests that the crystal structure is preserved throughout the film formation (Figure S6, Supporting Information). In addition, **TRI3** exhibited diffuse scattering in the high-angle region (≈4.4 Å), associated with the liquid-like interactions among the alkyl side chains. The lattice constant was deduced from the measured *d*-spacings and is gathered in Table S3 (Supporting Information).

After heating or shearing **TRI3**'s thin films, X-ray diffractograms showed the disappearance of the low-angle peaks, leaving only a broad, diffuse peak in the high-angle region (Figure 7c). Microscopic examination with crossed polarizers revealed an absence of birefringence. While this behavior might initially be interpreted as the amorphization of the thin films, detailed studies using polarized optical microscopy (POM) suggest that it is actually due to a shear-induced transition from a tetragonal columnar phase to a nematic discotic phase. Nematic discotic liquid crystals tend to form large domains that align homeotropically, explaining why the films appear transparent and lack birefringence under normal POM observation. However, when the sample is mechanically disturbed in the POM (i.e., disrupting their natural homeotropic alignment), birefringence becomes observable (Figure 7b).[51,52] While some liquid crystal phase transitions induced by mechanical shearing, transitioning from columnar to cubic phases, have been observed,[49,50,53–55] shear-induced transitions from a tetragonal to a discotic nematic phase have not been previously reported. It appears that under mechanical stress or heating the positional order in columns of the tetragonal columnar arrangement is disrupted (and therefore the favorable arrangement leading to the formation of J-aggregates), giving rise to a mesophase characterized only by orientational order. In the more fluid and disordered nematic mesophase, other types of aggregates can be found, such as excimers or exciplexes[56] explaining the emergence of red-shifted structureless bands, while the presence of isolated molecules can explain the presence of a band in the range of the monomer's absorbance. With time **TRI3** tends to crystallize again which explains the recovery of the fluorescence color (Figure S7, Supporting Information).

Interestingly, the liquid crystal behavior of **TRI3** varies depending on the cooling procedure from the isotropic phase. As noted earlier, the LC phase of **TRI3**, formed directly from thin films prepared by blade coating on glass slides, is a tetragonal columnar phase. Similarly, a tetragonal columnar phase can be obtained by slow cooling from the isotropic phase at a rate less than 1 °C min^{-1} as could be determined by POM. Rapid cooling of **TRI3** from the isotropic phase to room temperature leads to the formation of a discotic nematic phase. Please note that these transitions cannot be observed by DSC upon cooling.

2.4. Thermoresponsive Luminescent Inks and Self-Standing Labels

The stimuli-responsive behavior exhibited by **TRI3** renders it very attractive for potential applications as security inks. To progress toward such an application, we have investigated if the stimuli-responsive behavior is maintained on paper. To achieve that goal we prepared a **TRI3** (0.5 wt.%) solution in CH_2Cl_2, that was used as an ink to write on paper with the help of a cotton swap (**Figure 8**). Interestingly on paper, the compound not only maintained its thermal responsiveness, but also the reversibility of the process. When visualized under a UV lamp, the message painted presents the greenish emission color typical of the crystalline phase, but upon heating it turns orange and spontaneously reverses to the original color after some minutes.

The integration of stimuli-responsive materials within a polymer matrix is a simple strategy to fabricate smart self-standing labels.[57] We have incorporated **TRI3** in different

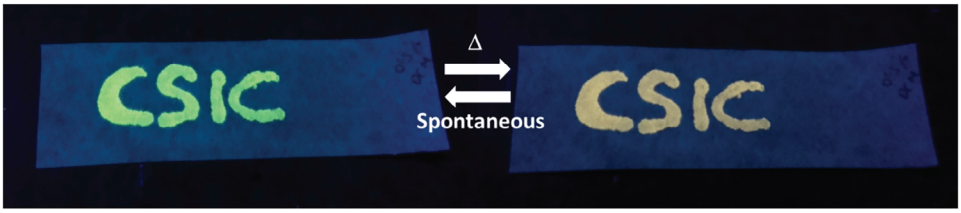

Figure 8. Message written on paper using a **TRI3** (0.5 wt.%) solution in CH_2Cl_2 as an ink, showing the change of color emission after heating, visualized under a UV lamp (356 nm).

polymeric matrices, including organic solvent soluble matrices, as polycarbonate (PC) and polysulfone (PSU) and water-soluble matrix as polyvinyl alcohol (PVA)in an attempt to confer the stimuli-responsive behavior to the resulting polymeric films.

Blends were prepared by adding 0.5% weight of compound **TRI3** to a solution of the corresponding polymer. PC and PSU matrices show a homogeneous distribution of the chromophore within itself. These blends show a fluorescence emission at ≈460 nm, which is very close to the emission of compound **TRI3** in solution (Figure S10, Supporting Information).

In contrast, when PVA is employed as a polymer matrix, a 500 nm emission blend is obtained (**Figure 9a**) associated with the J-aggregation. POM examination of this film under a polarizing optical microscope (Figure 9c) allowed us to detect the formation of microcrystals embedded in the polymeric matrix. In this case, the confinement in the PVA polar protic polymeric matrix favors the growth and retention of the crystalline phase within it, as has been previously observed in other luminophores.[57]

By heating the film, under a hot stage we observed a transformation in the color emission to brownish (Figure 9b,d) as previously observed in films on glass. However, in this case, no reversibility was observed when cooling back the doped polymer matrix at room temperature. This irreversible behavior makes this material interesting for applications such as temperature-sensitive labels or temperature safety indicators.

3. Conclusion

In this paper, we present **TRI3**, a stimuli-responsive fluorophore consisting of two trindole units endowed with long flexible chains, connected through a diacetylene bridge. The light-emitting properties of this compound drastically change under the influence of heat or pressure, which triggers a reversible phase transition between a tetragonal columnar and a discotic nematic liquid crystal phase. The mechanism behind the color

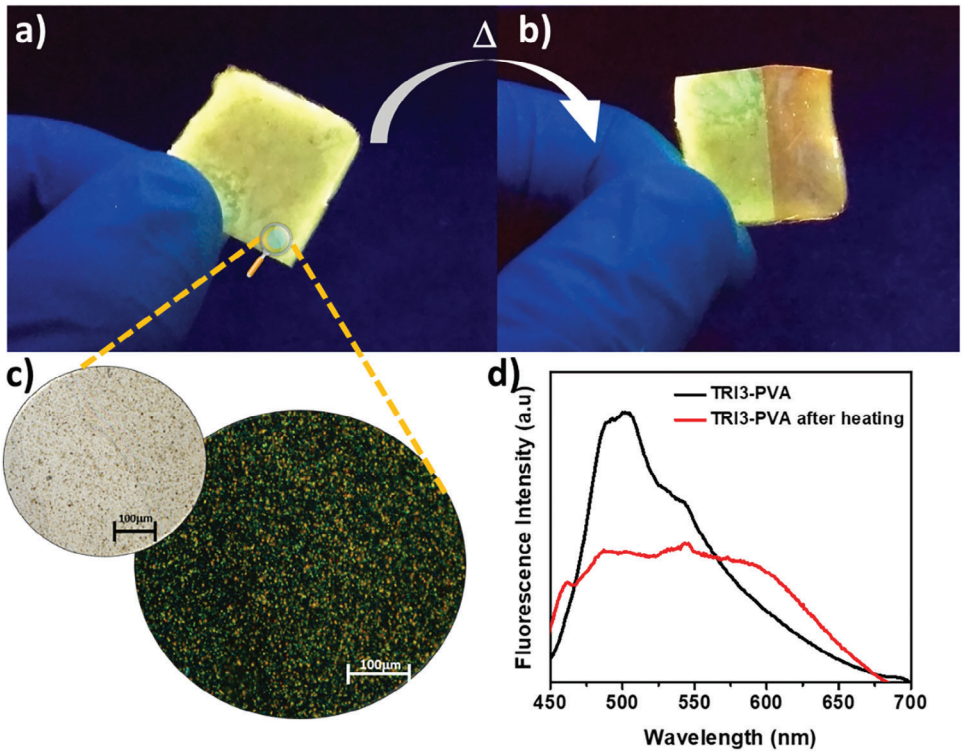

Figure 9. a) **TRI3**-PVA blend thin film at 356 nm UV light, b) **TRI3**-PVA blend thin film after heating half of it. c) Optical microphotographs of 0.5 wt.% of **TRI3** in the PVA film under visible and polarized light. d) Solid fluorescence spectrum of the **TRI3**-PVA blend before and after heating.

change has been attributed to the disruption of J-aggregates under the phase transformation.

Notably, the compound not only retains its thermal responsiveness on paper but also demonstrates the spontaneous reversibility of the process, making it particularly interesting for applications like rewritable paper, optical recording, or third-generation security inks. Conversely, when this material is incorporated into a PVA matrix to form self-standing hybrid films, it maintains its thermal responsiveness but loses the ability for reversion. This result broadens the potential applications of the material, especially in areas such as temperature-sensitive labels or safety indicators.

Supporting Information

Supporting Information is available from the Wiley Online Library or from the author.

Acknowledgements

This research was funded by MCIN/AEI/ 10.13039/501100011033 and by the "European Union NextGenerationEU/PRTR" (PDC2021-121002-I00, PID2023-150022NB-I00, PID2022-139548NB-I00, PID2023-146811NA-I00 and CEX2023-001286-S) by Junta de Andalucía (P09FQM-4708 and P18-FR-4559) and Gobierno de Aragón-FSE (E47_23R). R. Martín acknowledges the Spanish Ministry of Universities for a Margarita Salas postdoctoral fellowship under the agreement UNI/551/2021.A. Concellón is grateful for grant RYC2021-031154-I funded by MICIU/AEI/10.13039/501100011033 and by European Union NextGenerationEU/PRTR. We acknowledge support of the publication fee by the CSIC Open Access Publication Support Initiative through its Unit of Information Resources for Research (URICI). The authors would like to thank the computer resources, technical expertise, and assistance provided by the SCBI (Supercomputing and Bioinformatics). The authors also thank J. Perles and M. Ramirez for their collaboration in solving the crystal structure.

Conflict of Interest

The authors declare no conflict of interest.

Data Availability Statement

The data that support the findings of this study are available in the supplementary material of this article.

Keywords

anti-counterfeiting inks, J-aggregates, luminescence, stimuli-responsive, triazatruxene, triindole

Received: October 9, 2024
Revised: October 23, 2024
Published online:

[1] X. Yu, H. Zhang, J. Yu, *Aggregate* **2021**, *2*, 20.
[2] H. Zhang, D. Hua, C. Huang, S. K. Samal, R. Xiong, F. Sauvage, K. Braeckmans, K. Remaut, S. C. De Smedt, *Adv. Mater.* **2020**, *32*, 1905486.
[3] Z. Chen, H. Zhu, J. Qian, Z. Li, X. Hu, Y. Guo, Y. Fu, H. Zhu, W. Nai, Z. Yang, D. Li, L. Zhou, *Photonics* **2023**, *10*, 1014.
[4] L. E. MacKenzie, R. Pal, *Nat. Rev. Chem.* **2020**, *5*, 109.
[5] R. Feng, X. Bai, Y. Zi, Y. Song, H. Zhao, Y. Cun, Y. Liu, J. Qiu, Z. Song, A. Huang, Z. Xu, Z. Yang, *Adv. Opt. Mater.* **2024**, *12*, 2301293.
[6] X. Wang, F. Yan, M. Xu, J. Ning, X. Wei, X. Bai, *J. Colloid Interface Sci.* **2024**, *653*, 1137.
[7] K. Muthamma, D. Sunil, P. Shetty, *Appl. Mater. Today* **2021**, *23*, 101050.
[8] H. Zhou, J. Han, J. Cuan, Y. Zhou, *Chem. Eng. J.* **2022**, *431*, 134170.
[9] Y. Weng, Y. Hong, J. Deng, S. Cao, L.-J. Fan, *J. Colloid Interface Sci.* **2024**, *655*, 622.
[10] L. Wang, W. Zhong, W. Gao, W. Liu, L. Shang, *Chem. Eng. J.* **2024**, *479*, 147490.
[11] G. Huang, Q. Xia, W. Huang, J. Tian, Z. He, B. S. Li, B. Z. Tang, *Angew. Chem., Int. Ed.* **2019**, *58*, 17814.
[12] H. Mardani, H. Roghani-Mamaqani, S. Shahi, D. Roustanavi, *ACS Appl. Polym. Mater.* **2023**, *5*, 1092.
[13] X. Qiao, L. Kasim, A. Tuerdi, G. Hu, A. Abdukayum, *ACS Appl. Nano Mater* **2023**, *6*, 20831.
[14] H. Sun, S. Liu, W. Lin, K. Y. Zhang, W. Lv, X. Huang, F. Huo, H. Yang, G. Jenkins, Q. Zhao, W. Huang, *Nat. Commun.* **2014**, *5*, 3601.
[15] V. K. Praveen, B. Vedhanarayanan, A. Mal, R. K. Mishra, A. Ajayaghosh, *Acc. Chem. Res.* **2020**, *53*, 496.
[16] S. Cherumukkil, G. Das, R. P. N. Tripathi, G. V. PavanKumar, S. Varughese, A. Ajayaghosh, *Adv. Funct. Mater.* **2022**, *32*, 2109041.
[17] R. Thirumalai, R. D. Mukhopadhyay, V. K. Praveen, A. Ajayaghosh, *Sci. Rep.* **2015**, *5*, 9842.
[18] J. R. Lakowicz, *Principles of fluorescence spectroscopy*, 3rd Ed., Springer, New York **2006**.
[19] S. Varughese, *J. Mater. Chem. C* **2014**, *2*, 3499.
[20] M. Kasha, *Radiat. Res.* **1963**, *20*, 55.
[21] S. Xu, H.-W. Liu, S.-Y. Huan, L. Yuan, X.-B. Zhang, *Mater. Chem. Front.* **2021**, *5*, 1076.
[22] M. Más-Montoya, R. A. J. Janssen, *Adv. Funct. Mater.* **2017**, *27*, 1605779.
[23] T. Li, J. Benduhn, Z. Qiao, Y. Liu, Y. Li, R. Shivhare, F. Jaiser, P. Wang, J. Ma, O. Zeika, D. Neher, S. C. B. Mannsfeld, Z. Ma, K. Vandewal, K. Leo, *J. Phys. Chem. Lett.* **2019**, *10*, 2684.
[24] M. Su, S. Li, H. Zhang, J. Zhang, H. Chen, C. Li, *J. Am. Chem., Soc.* **2019**, *141*, 402.
[25] Z. Man, Z. Lv, Z. Xu, Q. Liao, J. Liu, Y. Liu, L. Fu, M. Liu, S. Bai, H. Fu, *Adv. Funct. Mater.* **2020**, *30*, 2000105.
[26] D. Yan, Z. Wang, Z. Zhang, *Acc. Chem. Res.* **2022**, *55*, 1047.
[27] H. K. Bisoyi, Q. Li, *Chem. Rev.* **2022**, *122*, 4887.
[28] C. Ruiz, E. M. García-Frutos, D. A. Da Silva Filho, J. T. López Navarrete, M. C. Ruiz Delgado, B. Gómez-Lor, *J. Phys. Chem. C* **2014**, *118*, 5470.
[29] S. Van Cleuvenbergen, I. Asselberghs, E. M. García-Frutos, B. Gómez-Lor, K. Clays, J. Pérez-Moreno, *J. Phys. Chem. C* **2012**, *116*, 12312.
[30] L. Ji, Q. Fang, M. Yuan, Z. Liu, Y. Shen, H. Chen, *Org. Lett.* **2010**, *12*, 5192.
[31] Y.-C. Hu, Z.-L. Lin, T.-C. Huang, J.-W. Lee, W.-C. Wei, T.-Y. Ko, C.-Y. Lo, D.-G. Chen, P.-T. Chou, W.-Y. Hung, K.-T. Wong, *Mater. Chem. Front.* **2020**, *4*, 2029.
[32] C. Coya, C. Ruiz, Á. L. Álvarez, S. Álvarez-García, E. M. García-Frutos, B. Gómez-Lor, A. De Andrés, *Org. Electron.* **2012**, *13*, 2138.
[33] J. Zhang, L. Gong, X. Zhang, M. Zhu, C. Su, Q. Ma, D. Qi, Y. Bian, H. Du, J. Jiang, *Chem., Eur. J.* **2020**, *26*, 13842.
[34] Y. Xu, X. Wu, Y. Chen, H. Hang, H. Tong, L. Wang, *RSC Adv.* **2016**, *6*, 31915.

[35] X.-C. Li, C.-Y. Wang, Y. Wan, W.-Y. Lai, L. Zhao, M.-F. Yin, W. Huang, *Chem. Commun.* **2016**, *52*, 2748.
[36] M. Echeverri, C. Ruiz, B. Gómez-Lor, *CrystEngComm* **2021**, *23*, 5925.
[37] C. Ruiz, J. T. López Navarrete, M. C. Ruiz Delgado, B. Gómez-Lor, *Org. Lett.* **2015**, *17*, 2258.
[38] F. C. Spano, *Acc. Chem. Res.* **2010**, *43*, 429.
[39] S. Pascal, S. Denis-Quanquin, F. Appaix, A. Duperray, A. Grichine, B. L.e Guennic, D. Jacquemin, J. Cuny, S.-H. Chi, J. W. Perry, B. Van Der Sanden, C. Monnereau, C. Andraud, O. Maury, *Chem. Sci.* **2017**, *8*, 381.
[40] J. Chen, L. Xiong, L. Zhang, X. Huang, H. Meng, C. Tan, *Chem. Phys. Lett.* **2020**, *747*, 137328.
[41] S. Dineshkumar, I. R. Laskar, *Polym. Chem.* **2018**, *9*, 5123.
[42] J. Chen, B. Z. Tang, *Aggregation-Induced Emission: Fundamentals* (Eds: A. Qin, B. Z. Tang), John Wiley and Sons Ltd, Chichester, United Kingdom **2013** p. 307.
[43] N. L. C. Leung, N. Xie, W. Yuan, Y. Liu, Q. Wu, Q. Peng, Q. Miao, J. W. Y. Lam, B. Z. Tang, *Chem., Eur. J.* **2014**, *20*, 15349.
[44] F. Würthner, T. E. Kaiser, C. R. Saha-Möller, *Angew. Chem., Int. Ed.* **2011**, *50*, 3376.
[45] E. M. García-Frutos, G. Hennrich, E. Gutierrez, A. Monge, B. Gómez-Lor, *J. Org. Chem.* **2010**, *75*, 1070.
[46] F. Gallego-Gómez, E. M. García-Frutos, J. M. Villalvilla, J. A. Quintana, E. Gutierrez-Puebla, A. Monge, M. A. Díaz-García, B. Gómez-Lor, *Adv. Funct. Mater.* **2011**, *21*, 738.
[47] C. Ruiz, U. K. Pandey, R. Termine, E. M. García-Frutos, G. López-Espejo, R. P. Ortiz, W. Huang, T. J. Marks, A. Facchetti, M. C. Ruiz Delgado, A. Golemme, B. Gómez-Lor, *ACS Appl. Mater. Interfaces* **2016**, *8*, 26964.
[48] C. Ruiz, I. Arrechea-Marcos, A. Benito-Hernández, E. Gutierrez-Puebla, M. A. Monge, J. T. López Navarrete, M. C. Ruiz Delgado, R. P. Ortiz, B. Gómez-Lor, *J. Mater. Chem. C* **2017**, *6*, 50.
[49] Y. Sagara, S. Yamane, T. Mutai, K. Araki, T. Kato, *Adv. Funct. Mater.* **2009**, *19*, 1869.
[50] K. P. Gan, M. Yoshio, T. Kato, *J. Mater. Chem. C* **2016**, *4*, 5073.
[51] A. Concellón, M. Marcos, P. Romero, J. L. Serrano, R. Termine, A. Golemme, *Angew. Chem.* **2017**, *129*, 1279.
[52] A. Concellón, R. Termine, A. Golemme, P. Romero, M. Marcos, J. L. Serrano, *J. Mater. Chem. C* **2019**, *7*, 2911.
[53] Y. Sagara, T. Kato, *Angew. Chem., Int. Ed.* **2008**, *47*, 5175.
[54] Y. Sagara, T. Kato, *Nat. Chem.* **2009**, *1*, 605.
[55] M. Mitani, S. Ogata, S. Yamane, M. Yoshio, M. Hasegawa, T. Kato, *J. Mater. Chem. C* **2016**, *4*, 2752.
[56] Note that triazatruxene molecules have a strong tendency to form exciplex systems due to associative interactions between excited and ground state molecules. See ref. 28.
[57] M. Echeverri, C. Ruiz, S. Gámez-Valenzuela, M. Alonso-Navarro, E. Gutierrez-Puebla, J. L. Serrano, M. C. Ruiz Delgado, B. Gómez-Lor, *ACS Appl. Mater. Interfaces* **2020**, *12*, 10929.